*17th World Conference on Earthquake Engineering, 17WCEE*
*Sendai, Japan - September 13th to 18th 2020*

# HYBRID SIMULATION OF A SELF-CENTERING BRIDGE-BENT AND COMPARISON WITH SHAKING TABLE TESTS

Y. Wu(1), K. M. Mosalam(2), S. Günay(3), A. Nema(4), and J. I. Restrepo(5)

(1) *Ph.D. Candidate, Dept. of Civil & Environmental Engineering, Univ. of California, Berkeley. yingjie_wu@berkeley.edu*
(2) *Taisei Professor of Civil Engineering and Director of the Pacific Earthquake Engineering Research (PEER) Center, Dept. of Civil & Environmental Engineering, Univ. of California, Berkeley. mosalam@berkeley.edu*
(3) *Project Scientist, Dept. of Civil & Environmental Engineering, Univ. of California, Berkeley. selimgunay@berkeley.edu*
(4) *Post Doc Researcher, The Pacific Earthquake Engineering Research (PEER) Center, Univ. of California, Berkeley. anema@berkeley.edu*
(5) *Professor, Dept. of Structural Engineering, Univ. of California, San Diego. jrestrepo@ucsd.edu*

## Abstract

This study presents hybrid simulation (HS) tests conducted on a 1/3 scale two-column bridge bent with self-centering columns. The comparison of the HS tests with previously conducted shaking table tests on an identical bridge bent is one of the highlights of this study. The design of the bridge bent columns is characterized by a well-balanced combination of self-centering, rocking and energy dissipating mechanism, leading to minimum damage and low levels of residual drifts. In order to conduct the HS tests, a new hybrid simulation system (HSS) was developed, utilizing commonly available software and hardware components in most structural laboratories, namely, a computational platform using Matlab/Simulink, the interface hardware/software platform dSPACE, and MTS controllers and data acquisition system for the utilized actuators and sensors. The operation of the HSS is verified using several trial runs without the test specimen.

In the conducted HS tests, the two-column bridge bent was simulated as the experimental substructure while modeling the horizontal and vertical masses and the corresponding mass proportional damping in the computer. The same ground motions, consisting of one horizontal and the vertical components, used in the shaking table tests, were applied as input excitations to the equations of motion in the HS. Good matching was obtained between the shaking table and the HS test results, demonstrating the correctness of the defined governing equations of motion and the employed damping model, in addition to the reliability of the developed HS system with minimum simulation errors. The small residual drifts and the minimum level of structural damage at large peak drift levels demonstrated the superior seismic response of the innovative design of the bridge bent with self-centering columns. The reliability of the developed HS approach is motivating a follow-up HS study where the entire two-span bridge deck and its abutments represent the computational substructure while the two-column bridge bent is still the physical substructure. This is expected to shed more light on the performance of the tested innovative bridge bent design beyond what can be achieved via shaking table tests, which limit large-scale bridge system investigation.

*Keywords: Bridges; Energy dissipation; Hybrid simulations; Self-centering; Shaking table experiments.*

## 1. Introduction

Bridges often serve as key links in the local and national transportation networks, and any closures will have severe costs not only for repair or replacement, but also in the form of economic losses and other consequences related to medium and long-term interruption of businesses, disruption of communities and difficulty in the emergency response operations. Considering the importance of these structures, the design philosophy is now shifting from collapse prevention to maintaining functionality in the aftermath of moderate to strong earthquakes. In addition to performance, the construction philosophy is also being modernized with the utilization of Accelerated Bridge Construction (ABC) techniques to reduce impacts on traffic, society, economy and on-site safety during construction.

The research presented in this paper is part of a study that investigates the system level response of bridges with enhanced response features including self-centering, rocking, confinement and energy-dissipation. For this purpose, a 1/3 scale two-column bridge bent with enhanced response features was designed and subjected to a series of shaking table tests [1]. As a result of the conducted shaking table tests, the bridge bent was observed to experience good seismic performance with very small residual drifts. The objective of an accompanying study was to explore whether similar good performance could be achieved when the complete bridge response was considered using hybrid simulation (HS). This accompanying study was conducted in two phases, in the first phase a hybrid simulation system was developed and HS tests were conducted with this system on an identically constructed bridge bent and the HS test results were compared against the shaking table tests to validate the considered hybrid simulation approach and the developed hybrid simulation system Second phase was related to the HS tests conducted on a complete bridge with columns of enhanced response features. This paper provides background information on the bridge bent with enhanced response features and the conducted shaking table tests and explains the developed hybrid simulation system, conducted HS tests and comparison with the shaking table test results.

## 2. System Description

The developed bridge subsystem, Fig. 1, combines precast post-tensioned columns with precast foundation and cap beams to simplify off- and onsite construction burdens and minimize earthquake-induced damage and associated repair costs. Each column consists of reinforced concrete cast inside a segmented cylindrical steel jacket, which acts as both the formwork and confinement to concrete and serves as transverse reinforcement. The pre-cast end beams have corrugated duct lined sockets, where the columns will be placed and grouted on-site to form the column-beam joints. Large inelastic deformation demands in the structure are concentrated at the column-beam interfaces, which are designed to accommodate these demands with minimal structural damage through rocking behavior. Longitudinal post-tensioned high strength steel threaded bars, designed to respond elastically, ensure re-centering behavior. Internal mild steel rebars, debonded from the concrete at the interfaces, provide energy dissipation and impact mitigation.

## 3. Shaking Table Tests Summary

### 3.1 Specimen Description

The developed system was tested on the PEER 6-DOF shaking table in 2017. The prototype bent used in the planning of these tests was derived from an existing bridge: the Massachusetts Avenue Over Crossing (MAOC) located in San Bernardino, California near the I215/HW210 interchange in close proximity to the San Andreas Fault. To maximize the utilization of the shaking table in terms of force and displacement capacities, and to optimize the experimental cost, only the two edge columns in bent #3 were used. The distance between the columns was adjusted to maintain the same level of column axial load and the columns of the prototype bent were redesigned to incorporate the innovative design features, Fig. 2. Resulting prototype bent was further scaled by 1/3 to accommodate the shaking table capacities



© The 17th World Conference on Earthquake Engineering - 2d-0084 -

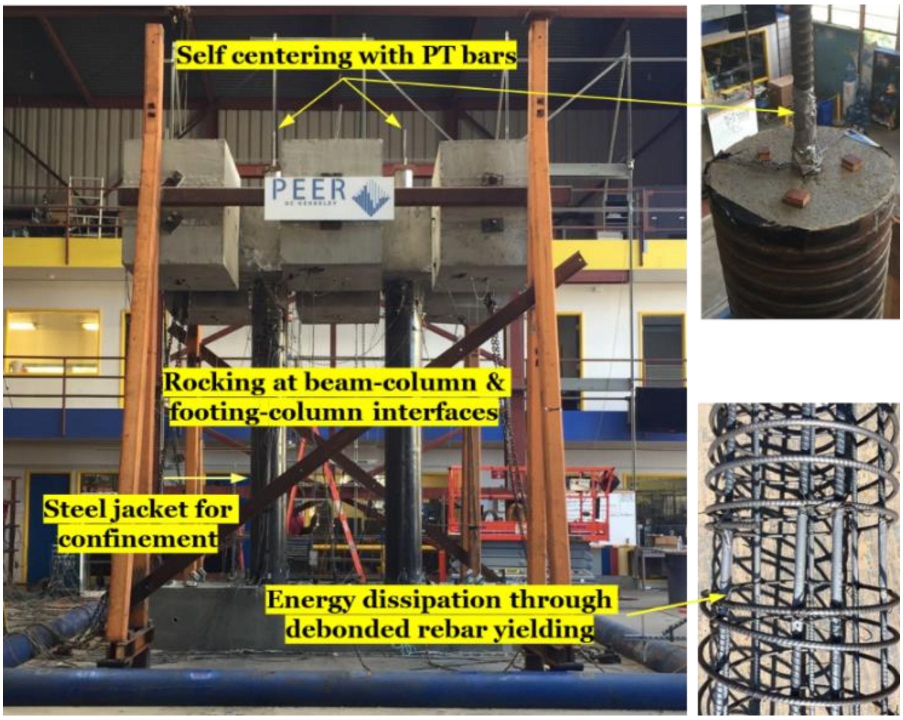


Fig. 1 – Innovative design features of the investigated bridge subsystem.

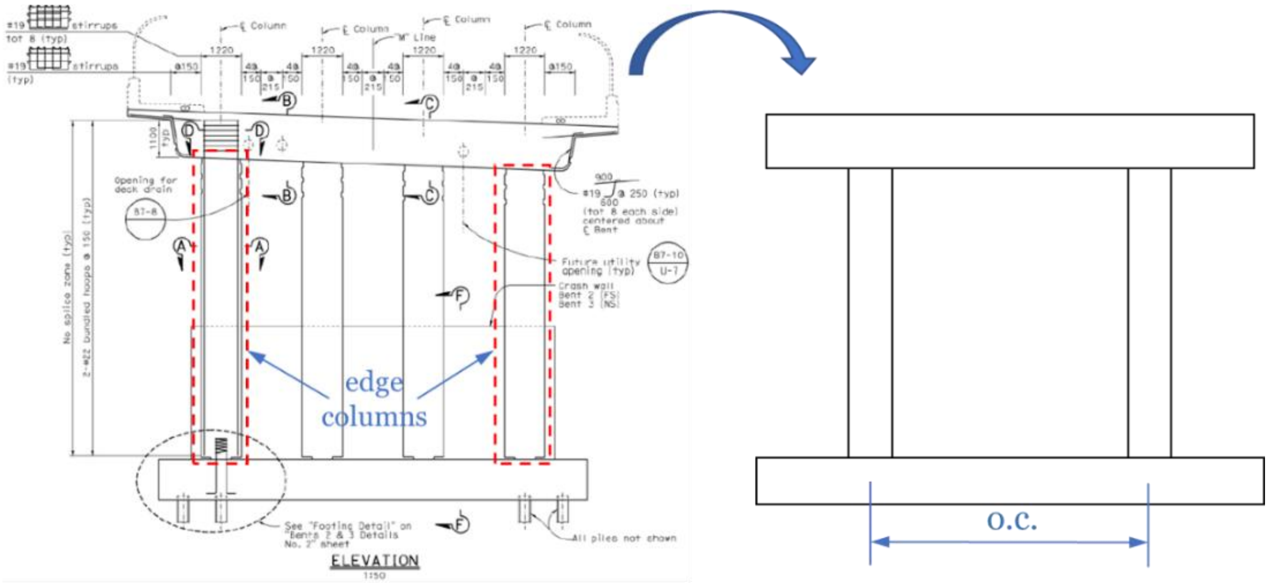


MAOC bent #3 prototype bent

Fig. 2 – Prototype bent derived from the MAOC bridge.

In the shaking table tests, inertia forces were provided by six concrete blocks post-tensioned to the cap beam for a combined weight of 69 kips, simulating a portion of the bridge superstructure over two columns. Fig. 3 shows the setup and specimen configuration in the shaking table test. Several ground motions, with one horizontal and one vertical component, were applied and ground motions are selected and scaled according to targeted lateral displacement demands as predicted by preliminary numerical simulations.



© The 17th World Conference on Earthquake Engineering 

Fig. 3 – Test setup used in the shaking table test.

### 3.2 Input Ground Motions

The ground motion selection was made based on expected peak drift from the numerical simulation, in comparison with the design drift capacity of system defined by the yielding of the PT bars and calculated to be 7%. The selected motions represent very small (0.6% drift), small (1.8% drift), moderate (4% drift) and large (>5% drift) events. Nine ground motions were planned in the initial loading protocol. To investigate the effect of lower intensity aftershocks, the test was not conducted with continuously increasing demands; instead, a larger motion was followed by smaller intensity of shaking until a peak drift of 4% was reached. For larger drifts, ground motion polarity was occasionally switched to avoid damaging the specimen in only one direction. Significant structural integrity remained after the initially planned sequence and the scope was expanded with three additional tests. Details of the ground motions are listed in Table 1 in the order that they were applied.

Table 1 – Input ground motion sequence for shaking table tests.

| EQ # | Event Name | Station Name | Unscaled PGA (g) | Scale Factor | Expected Drift (%) |
|---|---|---|---|---|---|
| 01 | Landers, 1992 | Lucerne | 0.72 | 0.9 | 0.6 |
| 02 | Landers, 1992 | Lucerne | 0.72 | 0.9 | 0.6 |
| 03 | Tabas, 1978 | Tabas | 0.85 | -0.9 | 1.8 |
| 04 | Kocaeli, 1999 | Yarimca | 0.3 | 1 | 0.6 |
| 05 | Northridge, 1994 | RRS | 0.85 | 0.81 | 4 |
| 06 | Duzce, 1999 | Duzce | 0.51 | 1 | 1.8 |
| 07 | Northridge, 1994 | NFS | 0.72 | -1.2 | 4 |
| 08 | Kobe, 1995 | Takatori | 0.76 | -0.8 | 5 |
| 09 | Kobe, 1995 | Takatori | 0.76 | 0.9 | 7 |
| 10 | Tabas, 1978 | Tabas | 0.85 | -0.9 | - |
| 11 | Northridge, 1994 | RRS | 0.85 | 0.81 | - |
| 12 | Kobe, 1995 | Takatori | 0.76 | -0.8 | - |

### 3.3 Test Results

The hysteretic responses during the tests are shown in Fig. 4. The lateral forces were normalized by the specimen inertia weight and expressed as base shear coefficients. The pinched shape or the “flag-shape” of



© The 17th World Conference on Earthquake Engineering 

hysteresis loop is the characteristic behavior of re-centering systems, with very small residual displacement but peak capacity comparable to that of a conventional ductile system.

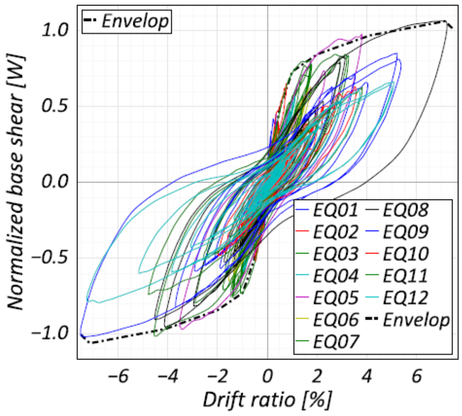


Fig. 4 – Overlaid hysteretic response for all runs.

## 4. Hybrid Simulation Tests

In the conducted HS, an identical test specimen with the same geometry, same reinforcement detailing and same construction sequence was utilized, except that the six mass blocks were treated analytically instead of being explicitly attached to the cap beam. Some details of the HS are discussed in the following.

### 4.1 Substructuring and Test Setup

The simulated hybrid structure is described in Fig. 5(a). The bridge bent with two self-centering columns was considered as the experimental substructure, while the inertia mass blocks attached to the top of the test specimen were removed and replaced by analytical mass modeled in the computer along with viscous damping. Considering the two-directional ground motion input in the shaking table tests and considering that the responses from these two directions can be represented by two independent and uncoupled differential equations of motion, the horizontal and the vertical degrees of freedom (DOF) were formulized separately.

Fig. 5(b) shows the test setup. The horizontal actuator applies calculated lateral displacements to the test specimen, while the vertical actuator takes care of both the gravity loading and the effect of the vertical ground motion. To prevent the test specimen from moving sideways, an out-of-plane restraint was exploited by welding a T-beam to three steel plates embedded inside the cap beam. The T-beam is allowed to slide frictionless on the lateral supporting system.

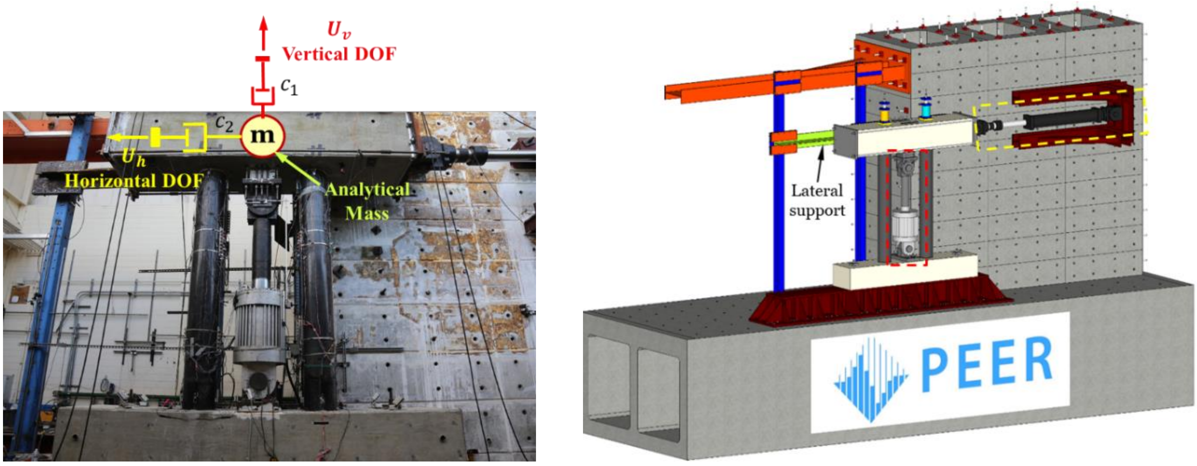


(a) (b)

Fig. 5 – (a) Substructuring in hybrid simulation; (b) hybrid simulation test setup.



© The 17th World Conference on Earthquake Engineering 

### 4.2 Hybrid Simulation System

Fig. 6 shows the newly developed hybrid simulation system. It consists of: (a) the computational platform Simulink which performs the numerical integration and the displacement interpolation; (b) dSPACE, an interface hardware/software platform which establishes the communication between the computational platform Simulink and the controller by performing digital to analog (D/A) and analog to digital (A/D) transformations and (c) two MTS 407 controllers that drive the vertical and the horizontal hydraulic actuators. It is noted that the hardware components of dSPACE is a DS1104 R&D Controller Board that was installed in the PCI slot of the host PC and the CP1104 Connector Panel with 8 ADC and 8 DAC channels. The Simulink model used in the computations is developed in the host PC and compiled on the DS1104 R&D Controller Board for deterministic (i.e. fixed sample timed) real-time execution. Software component of dSPACE is ControlDesk which provides an interface to the developed Simulink model.

For each numerical integration time step, two uncoupled SDOF equations were numerically solved in the Simulink model to compute the horizontal and the vertical displacements that are to be imposed to the specimen. The computed command displacements, after interpolation, were sent to the controller using a built-in DAC (digital to analog conversion) Simulink block that comes with dSPACE. The DAC block was used to convert the digital displacements to analog voltage that can be recognized by the controllers. After applying the computed displacements to the specimen, the corresponding reactions (resisting forces) were measured using load cells in each actuator and passed on to the controllers in analog voltages. The measured forces were sent to the computations in the Simulink model though another built-in Simulink block (analog to digital conversion, ADC block). The ADC block converted analog voltage to digital force values before passed on to the time stepping integration algorithm in Simulink to advance the solution to the next analysis step, Fig. 6.

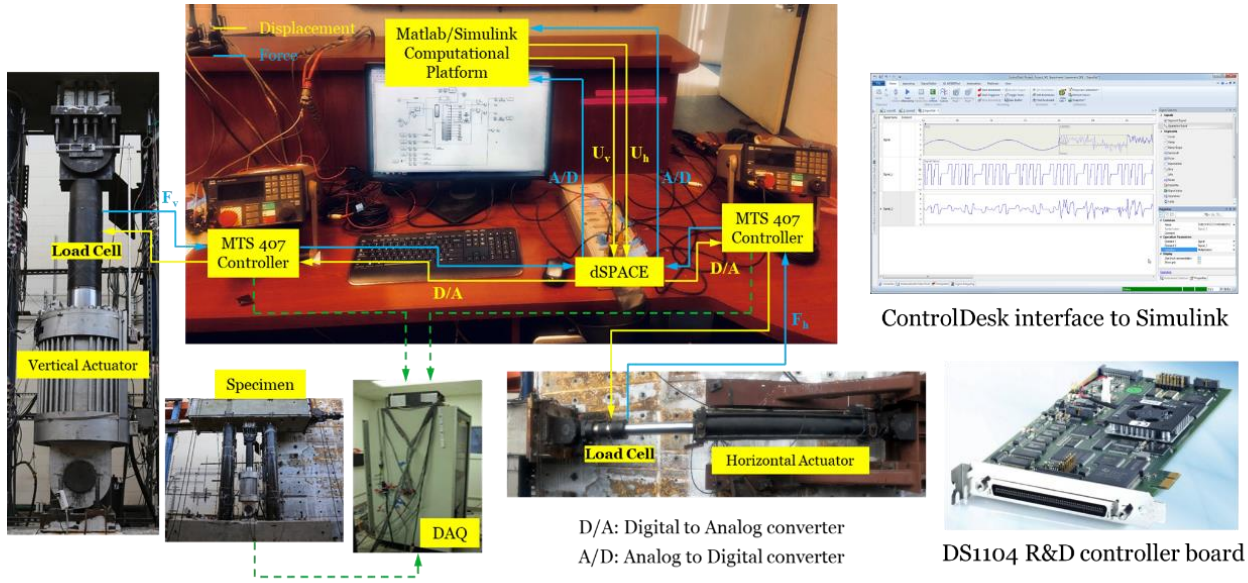


Fig. 6 – Main components and connectivity of the developed hybrid simulation system.

### 4.3 Numerical Integration

As mentioned before, two main tasks were accomplished on the Matlab/Simulink computational platform: numerical integration and displacement interpolation. One of the non-iterative numerical integration algorithms, namely the Explicit Newmark integration [2], was selected for its HS-compatible features [3]. The numerical integration for both DOFs was performed through the Matlab function blocks in Simulink. A typical numerical integration block is shown in Fig. 7, together with the detailed execution steps. The function block takes as inputs the mass $\boldsymbol{m}$, the damping coefficient $\boldsymbol{c}$, the ground acceleration (in the unit of in./s$^2$) at current time step $i$, the Newmark velocity coefficient $\gamma$, the displacement $\boldsymbol{u}_i$ at current time step, the measured force $\boldsymbol{f}_i$ corresponding to $\boldsymbol{u}_i$, the discrete time step $dt$, and the velocity $\dot{\boldsymbol{u}}_{i-1}$ and acceleration $\ddot{\boldsymbol{u}}_{i-1}$ at previous time



© The 17th World Conference on Earthquake Engineering 

step *i*-1, and outputs the acceleration $\ddot{\boldsymbol{u}}_i$, the velocity $\dot{\boldsymbol{u}}_i$, the total acceleration at current time step *i* and the displacement $\boldsymbol{u}_{i+1}$ at next time step *i*+1. The calculated quantities from the current calculation were written and stored using the Simulink blocks "DataStoreWrite" and "DataStoreMemory", and were read by the Simulink block "DataStoreRead" for the next step calculation.

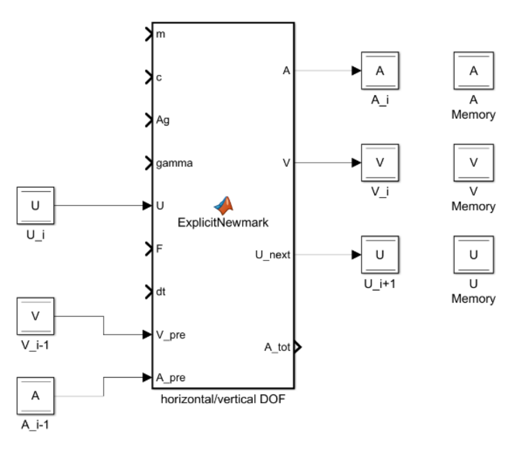


```
function [A,V,U_next,A_tot] =
ExplicitNewmark(m,c,Ag,gamma,U,F,dt,V_pre,A_pre)
% Expicit Newmark algorithm for SDOF system
% Inputs: m, c, Ag, gamma, U, F, dt, V_pre, A_pre
% Outputs: A, V, U_next, A_tot
% compute acceleration A at step i
P = -m*Ag;
m_eff = m + dt*gamma*c;
P_eff = P - F - c*(V_pre + dt*(1 - gamma)*A_pre);
A = P_eff/m_eff;
% compute velocity V at step i
V = V_pre + dt*((1 - gamma)*A_pre + gamma*A);
% compute displacement U_next at step i+1
U_next = U + dt*V +0.5*(dt^2)*A;
% compute total acceleration A_tot at step i
A_tot = A + Ag;
```

Fig. 7 – Matlab function block for Explicit Newmark numerical integration.

### 4.4 Displacement Interpolation

Between the current step displacement $\boldsymbol{u}_i$ and the next step displacement $\boldsymbol{u}_{i+1}$, interpolation of displacements was needed to generate commands for the controller. This is because the operation of the MTS 407 controller was based on receiving a command displacement at every 10 milliseconds and the hybrid simulation test was conducted slower than real time and the actuator velocity was limited to 0.05 in./s in order to achieve good control quality. Therefore, the maximum allowed displacement increment $\boldsymbol{u}_{incr}$ between two commands was 0.05 in./s × 10 millisecond = 0.0005 in. Simulink blocks used to determine the number of interpolations between the two integration time steps is shown in Fig. 8. In both horizontal and vertical directions, absolute values of the displacement increment between two adjacent steps were obtained and divided by the maximum allowed displacement increment $\boldsymbol{u}_{incr}$. Resulting two numbers were rounded up to the nearest integers and the largest of the two was picked to be the number of interpolation steps for both directions. The horizontal and vertical displacements were then linearly interpolated accordingly using the number of interpolation steps.

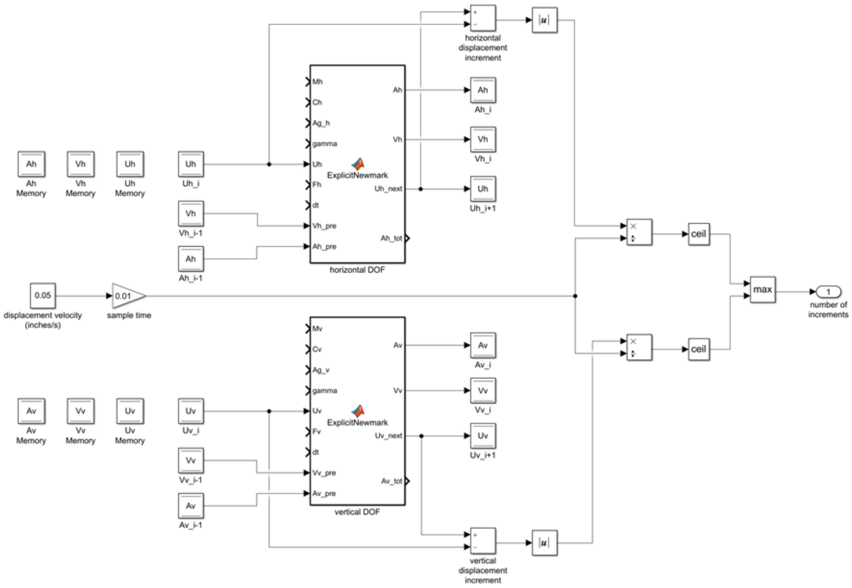


Fig. 8 – Simulink blocks for calculating the number of interpolation steps between two adjacent time steps.



© The 17th World Conference on Earthquake Engineering 

## 4.5 Loading

A gravity load of 47 kips, representing the gravity load from the six mass blocks, was applied before starting the hybrid simulation. The ground motion input for the HS were the accelerations measured by accelerometers mounted on the shaking table during the shaking table tests.

Fig. 9(a) shows the force-displacement relationship in the vertical direction during the gravity loading phase. There is a clear change in stiffness during gravity loading that can be observed from this plot. This was caused by compression of the grout between the top clevis connection anchorage of the vertical actuator and the surface of the cap beam, shown in Figs. 9(b) and (c). When the vertical actuator pulled down, it first squeezed the grout before starting to engage the complete vertical stiffness of the specimen. Therefore, the stiffness was small during the compression of the grout. After that, the vertical actuator started acting against the specimen and the response became much stiffer, representing the correct stiffness. In order to eliminate this problem due to the test setup, instead of displacement control, forces that were computed by multiplying the vertical displacements by the specimen vertical stiffness were directly applied in the vertical direction.


(a) (b) (c)

Fig. 9 – (a) Force-displacement plot during the gravity loading; (b) & (c) connection detailing of the vertical actuator's top clevis to the cap beam.

## 4.6 Hybrid Simulation Parameters

The parameters used in the hybrid simulation is chosen for proper representation of the dynamics of the two uncoupled SDOF systems. The response of a SDOF system in the linear elastic range is completely defined by its period and damping. To match the results from the shaking table test, it was important to identify the correct period and damping of the test specimen from the shaking table test. The test results from EQ2 of the shaking table test were used for this purpose because the specimen remained mostly in the linear elastic range of response during this test. EQ1 shaking table test was not considered here, since one of the inertia blocks was found to be not seated properly and the restraint frame was found to be bearing against the specimen, providing lateral resistance during EQ1, Fig. 3.

### 4.6.1 Horizontal direction

The period of the test specimen in the horizontal direction was investigated by taking the Fast Fourier Transformation (FFT) of the measured horizontal acceleration time history from the top of the specimen during the shaking table test EQ2. There were a total number of 16 accelerometers measuring the horizontal acceleration on top and the average value was considered. The FFT results is shown in Fig. 10(a). The frequency corresponding to the peak is 2.3 Hz, which results in the horizontal period to be 0.43 s.



© The 17th World Conference on Earthquake Engineering 

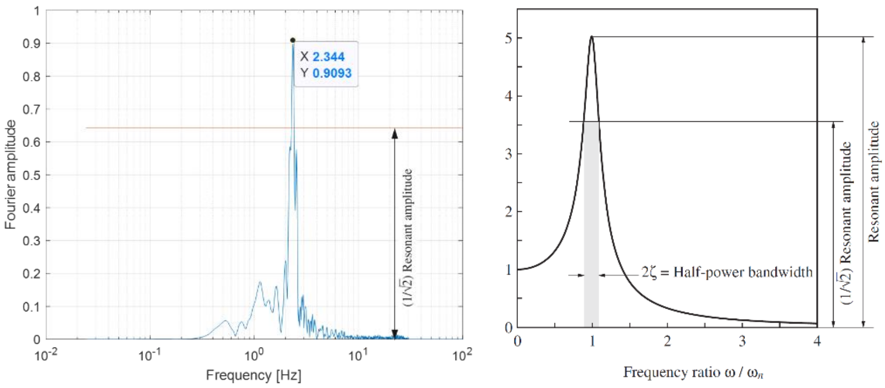


(a) (b)

Fig. 10 – (a) FFT and half-power bandwidth results in the horizontal direction; (b) half-power bandwidth method illustration [4].

The damping ratio was computed as 3% using the half-power bandwidth method [4]. Stiffness of the specimen was computed from a low-level test with two small cycles and the mass ***m*** and the damping coefficient ***c***, were computed to match the period and damping ratios identified from the shaking table tests. The horizontal inertia mass considered in the shaking table test includes six mass blocks, the cap beam and top half of the two columns, which results in a total mass of 68.18 kips/g, while the mass used in the HS tests was 81 kips/g. This was mainly because the HS tests were conducted one year after the shaking table tests, therefore the HS specimen had a larger stiffness compared to the shaking table specimen.

### 4.6.1 Vertical direction

To determine the parameters in the vertical direction, initially the method described above for the horizontal direction was adopted and vertical period and damping ratios were identified as 0.065s and 0.36%, where the identified damping ratio was questionable. Therefore, considering that the response in the vertical direction would remain essentially elastic, another approach was considered that sought the vertical direction parameters by matching the shaking table test results for EQ2. For this purpose, the response of a linear elastic SDOF system was investigated by varying the period and the damping ratio in a certain range. Investigated period and damping range were selected to be 0.04 s~0.08 s and 1%~15% respectively. The root-mean-square (RMS) error was computed by comparing the displacement response of the SDOF system against the shaking table test results and the parameter combination which yielded the smallest RMS error was selected. It was found that the period of 0.076 s and damping ratio of 11.1% gave the best match between the analysis and the shaking table results and used to compute the mass ***m*** and damping coefficient ***c*** in the vertical direction. It is noted that the damping ratio identified this way was higher than expected, however this was considered to be more realistic, especially considering the possible friction between the lateral supporting frame and the mass blocks during the shaking table test, Fig. 3.

## 4.7 Hybrid Simulation Verification Test

To confirm the performance of the implemented developments and validate the whole hybrid simulation system and proper actuator tracking, a HS verification test, or rehearsal, was indispensable. The rehearsal HS was conducted with a free actuator detached from the specimen, where the measured displacements were multiplied with a constant that represented the stiffness specimen and employed as the force feedback, Fig. 11.

The displacement time history obtained from the rehearsal HS using EQ2 was compared against the displacement time history obtained from a pure simulation conducted with the same mass, damping coefficient and stiffness used in the rehearsal HS. Perfect match between the pure simulation and the hybrid simulation rehearsal in Fig. 12 indicated proper functioning of the computations, communication between the HS components and proper actuator control and displacement tracking.



© The 17th World Conference on Earthquake Engineering 

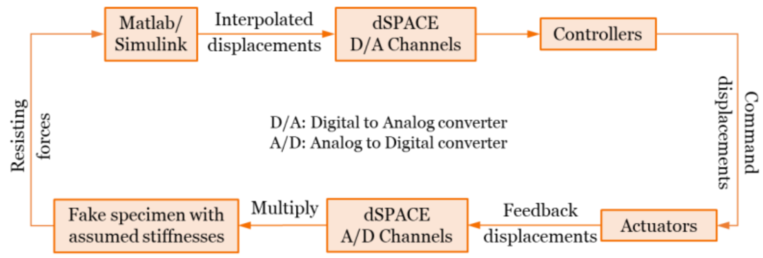


Fig. 11 – Schematic representation of the hybrid simulation rehearsal.

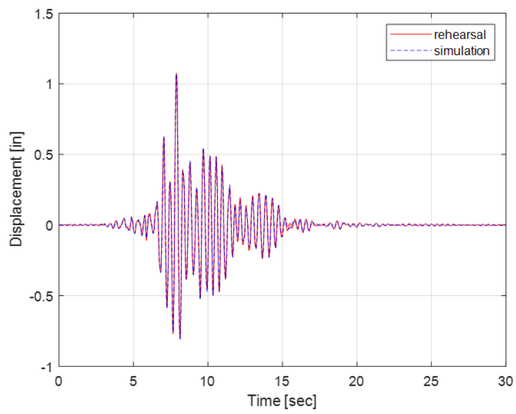


Fig. 12 – HS verification test in the horizontal direction.

## 5. Test Results

Six HS tests were conducted with EQ2 to EQ7 in Table 1 and compared against the shaking table test results. To increase the accuracy of the numerical integration, the shaking table ground motion records, which were originally recorded with a time step of 0.005s, were interpolated to reduce the time step from 0.005s to 0.001s. Figs. 14 to 17 show the time histories for displacement and acceleration and the force-displacement comparison between the shaking table and the hybrid simulation tests in the horizontal direction for EQ3, 4, 6 and 7. The results showed pretty good overall matching in terms of the amplitude of the response quantity, the time history pattern and the hysteretic behavior of the test specimen, although there were some discrepancies in some of the runs towards the end. This might be caused by two reasons: one is the possible friction force from the lateral support system in the HS setup; the other one might be the small levels of rate dependency of reinforced concrete [5]. Another observation is that the matching is better for large ground motions than small ones. Low levels of residual drift were observed in both the HS and shaking table tests, indicating the superior seismic response of the innovative design of the bridge bent with self-centering columns.

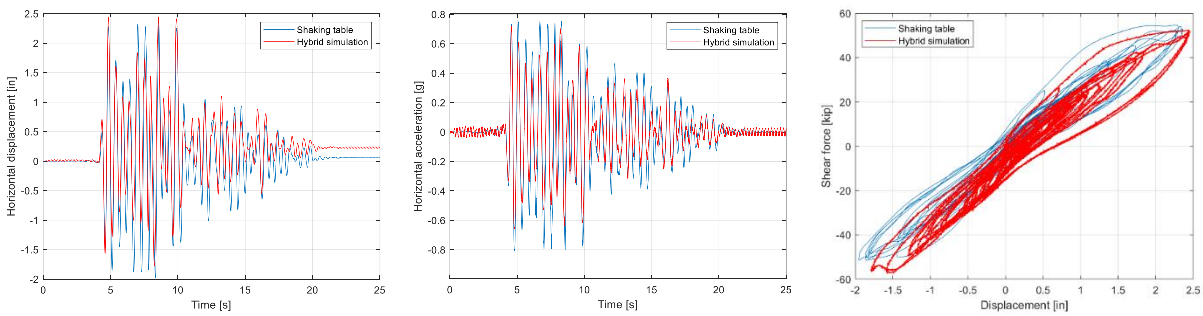


(a) (b) (c)

Fig. 11 – (a) Displacement time history; (b) acceleration time history; and (c) force-displacement relationship comparison of EQ3.



© The 17th World Conference on Earthquake Engineering 

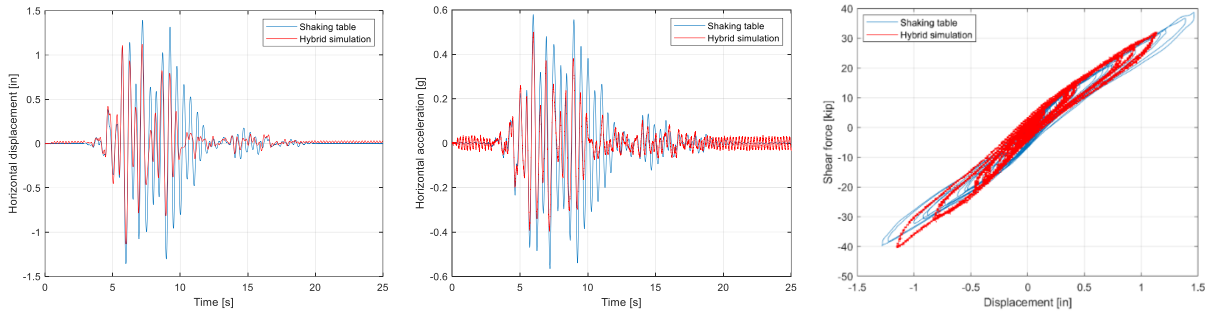


(a) (b) (c)

Fig. 12 – (a) Displacement time history; (b) acceleration time history; and (c) force-displacement relationship comparison of EQ4.

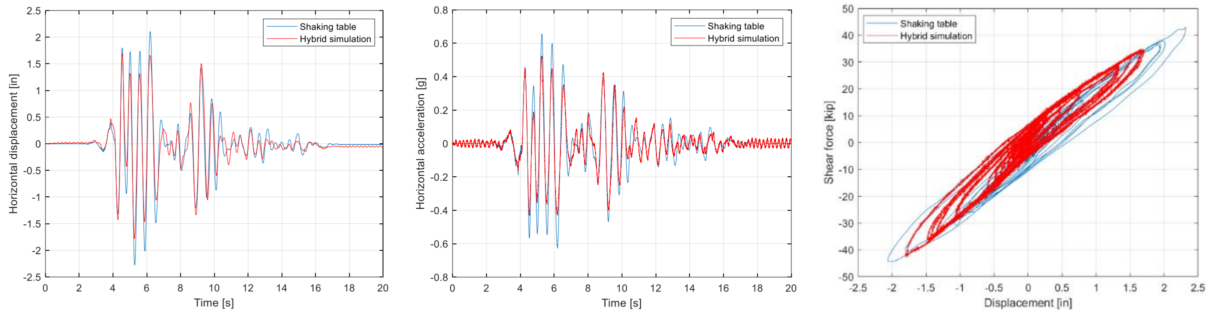


(a) (b) (c)

Fig. 13 – (a) Displacement time history; (b) acceleration time history; and (c) force-displacement relationship comparison of EQ6.

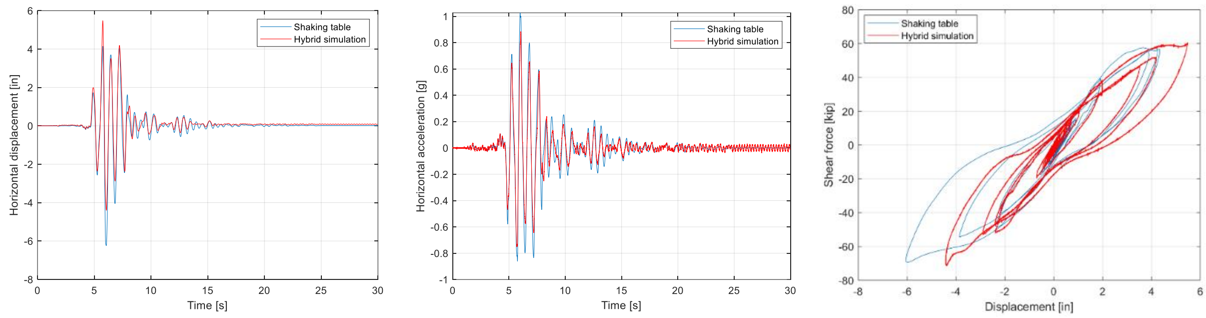


(a) (b) (c)

Fig. 14 – (a) Displacement time history; (b) acceleration time history; and (c) force-displacement relationship comparison of EQ7.

## 6. Summary and Conclusions

This study focused on the HS of a two-column bridge bent with innovative design features and the comparison of the HS results against the shaking table tests. A new hybrid simulation system (HSS) was designed, utilizing the computational platform Matlab/Simulink, the interface hardware/software platform dSPACE, and MTS controllers and data acquisition system for the utilized actuators and sensors. The operation of the HSS was verified by several trial runs without utilizing the test specimen.

HS results conducted for six ground motions were compared against the shaking table test results. Pretty good matching was achieved in terms of different response quantities. In addition, the residual drifts were observed to be as small as the shaking table tests, indicating the same conclusions were obtained from the two test types about the response of the explored self-centering bridge bent. These results justify the correctness of the defined equations of motion and the employed damping model, the minimum level of simulation errors



© The 17th World Conference on Earthquake Engineering 

and the reliability of the developed HSS. Matching of the HS and shaking table tests results is expected to increase confidence of HS in the testing of new structural/geotechnical systems.

## 7. Acknowledgements

The authors acknowledge the funding support from the PEER TSRP Program. The assistance from the PEER laboratory staff is highly appreciated.

## 8. References

[1] Nema, A. (2018). *Development of Low Seismic Damage Structural Systems.* PhD Dissertation, Department of Structural Engineering, University of California, San Diego.

[2] Newmark N.M. (1959). “A method of computation for structural dynamics.” *ASCE J. Eng. Mec*. 85: EM3 67-94.

[3] Mosalam, K.M., Günay S. (2014). "Seismic performance evaluation of high voltage disconnect switches using real-time hybrid simulation: I. System development and validation," *Earthquake Engineering and Structural Dynamics*, 43(8): 1205-1222.

[4] Chopra A.K. (2007). *Dynamics of Structures: Theory and Applications to Earthquake Engineering*, 3rd edition Prentice Hall: Englewood Cliffs, New Jersey.

[5] Moehle, J.P. (2014). *Seismic Design of Reinforced Concrete Buildings*, McGraw-Hill Eduation.



© The 17th World Conference on Earthquake Engineering 